Chaotic alternation of waves in ring lasers

M. Clerc and P. Coullet
INLN, 1361 Route des Lucioles, 06560 Valbonne, France

(Received 14 April 1999)

We intend to give an analytic description of the mechanisms involved in the periodic and chaotic wave alternation frequently observed in ring lasers. A set of amplitude equations is derived from the Maxwell-Bloch equations. These equations are studied analytically and numerically. [S1063-651X(99)03112-8]

PACS number(s): 05.45.−a, 42.60.Mi, 42.65.−k, 42.50.Md

I. INTRODUCTION

Ring lasers exhibit very interesting complex longitudinal dynamical behaviors [1–3]. The difficulty in analyzing these behaviors using simple equations is related to the fact that secondary instabilities occur very close to threshold [4]. In ring lasers, theoretical models predict stable traveling waves close to threshold. Although they are observed in experiments, their range of stability is quite narrow. Periodic and chaotic alternation of right- and left-traveling waves appears to be a more robust dynamical behavior in such a system [5–9]. A good qualitative understanding of the mechanism of alternation was carried out by using Galerkin approximations of the equations of Maxwell-Bloch for the class B lasers [10,11]. In this paper we intend to reduce asymptotically the Maxwell-Bloch equations to a simple set of quadratic amplitude equations. This model allows us to study in detail the mechanism of the transition from traveling waves to alternating waves and the nature of the chaotic behaviors itself. We first reduce the Maxwell-Bloch equations to the amplitude equations. The study of the elementary solutions and their codimension one and (two) bifurcations are considered in detail. A qualitative comparison with experiments in which the detuning is varied is presented.

II. FROM MAXWELL-BLOCH TO QUADRATIC AMPLITUDE EQUATIONS

The Maxwell-Bloch equations which describe the dynamics of longitudinal modes in ring lasers are given by [12]

$$\frac{\partial^2 E}{\partial t^2}=\frac{\partial^2 E}{\partial x^2}-\frac{\partial^2 P}{\partial t^2}-2\kappa\frac{\partial E}{\partial t},$$

$$\frac{\partial^2 P}{\partial t^2}=-2\gamma_\perp\frac{\partial P}{\partial t}-[\gamma_\perp^2+(1+\Delta)^2]P-gNE, \tag{1}$$

$$\frac{\partial N}{\partial t}=-\gamma_\parallel(N-D_0)+E\left(\frac{\partial P}{\partial t}+\gamma_\perp P\right),$$

where E, P, and N represent, respectively, the suitably normalized linearly polarized electric field, the corresponding polarization, and the population inversion. $\kappa,\gamma_\perp,\gamma_\parallel$, are the damping constants, Δ the detuning, g a constant which characterizes the atoms, and D_0 the pump parameter. Instability sets in when the pump exceeds a critical value $D_{0,c}\equiv 4\gamma_\perp\kappa/g\{1+[\Delta^2/2(\gamma_\perp+\kappa)^2]\}$.

Close enough to the onset, the amplitude equations obtained using the standard asymptotic analysis take the form of two coupled cubic Landau equations. The amplitudes of the right- and left-going waves are defined as

$$\begin{pmatrix}E\\P\\N\end{pmatrix}=\begin{pmatrix}0\\0\\D_{o,c}\end{pmatrix}+\frac{\epsilon}{2\sqrt{\kappa}}A(T)e^{i[(1+\omega_c)t-kx]}\times\begin{pmatrix}1\\-\dfrac{2\Delta\kappa}{(\kappa+\gamma_\perp)}+i2\kappa\\0\end{pmatrix}+\frac{\epsilon}{2\sqrt{\kappa}}B(T=\epsilon t)e^{i[(1+\omega_c)t+kx]}\times\begin{pmatrix}1\\-\dfrac{2\Delta\kappa}{(\kappa+\gamma_\perp)}+i2\kappa\\0\end{pmatrix}-\frac{\epsilon^2}{\gamma_\parallel}\begin{pmatrix}0\\0\\|A|^2+|B|^2\end{pmatrix}-\frac{\epsilon^2}{\gamma_\parallel}e^{i2kx}\begin{pmatrix}0\\0\\\bar{A}B\end{pmatrix}+o(\epsilon^3). \tag{2}$$

They obey the amplitude equations

$$\partial_t A=\tilde{\mu}A-\frac{e^{i\alpha}}{\gamma_\parallel}(|A|^2+2|B|^2)A,$$

$$\partial_t B=\tilde{\mu}B-\frac{e^{i\alpha}}{\gamma_\parallel}(|A|^2+2|B|^2)B, \tag{3}$$

where

$$\epsilon=N_0-N_{0,c},\omega_c=\frac{\Delta\kappa}{\kappa+\gamma_\perp}+\frac{b\epsilon}{a^2+b^2},\quad \tilde{\mu}\equiv\frac{a(D_0-D_{0,c})}{a^2+b^2}$$

$$a\equiv\frac{g(\gamma_\perp+\kappa)^3}{4\{(\gamma_\perp+\kappa)^4+[\Delta(\kappa-\gamma_\perp)]^2\}},\quad \tan\alpha=\frac{\Delta(\kappa-\gamma_\perp)}{(\gamma_\perp+\kappa)^2},$$

$$b\equiv\frac{\Delta g(\gamma_\perp^2-\kappa^2)}{4\{(\gamma_\perp+\kappa)^4+[\Delta(\kappa-\gamma_\perp)]^2\}}. \tag{4}$$

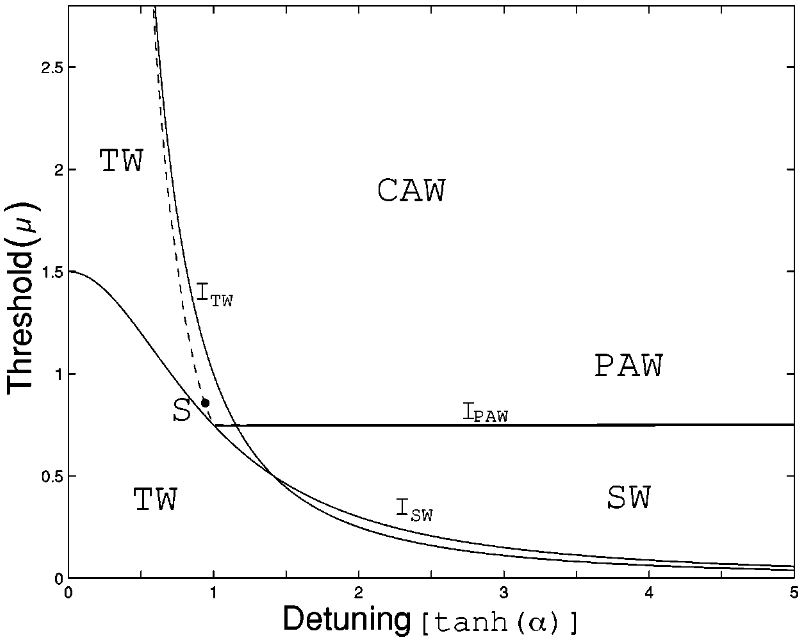

FIG. 1. Bifurcation diagram associated with Eq. (6). The solid lines correspond to the bifurcations of standing waves (I_{SW}), traveling waves (I_{TW}), and periodic alternating waves (I_{PAW}). The dotted line corresponds to the heteroclinic bifurcation which connects the two mixed waves.

For positive $\tilde{\mu}$, right-going and left-going waves are the only stable solutions of the coupled equations.

Amplitude equations which contain richer behaviors are obtained when $\gamma_\parallel$ is of the order ε. The bifurcation equations become quadratic and include then two new amplitudes N_0 and N_2,

$$\begin{pmatrix} E \\ P \\ N \end{pmatrix} = \begin{pmatrix} 0 \\ 0 \\ D_{0,c} \end{pmatrix} + \epsilon\gamma_\parallel (N_0 + N_2 e^{-i2kx}) \begin{pmatrix} 0 \\ 0 \\ 1 \end{pmatrix}$$
$$+ \frac{\epsilon}{\sqrt{\kappa\gamma_\parallel}} A\left(T = \frac{\epsilon}{\gamma_\parallel} t\right) e^{i[(1+\omega_c)t - kx]}$$
$$\times \begin{pmatrix} 1 \\ -\dfrac{2\Delta\kappa}{(\kappa+\gamma_\perp)} + i2\kappa \\ 0 \end{pmatrix}$$
$$+ \frac{\epsilon}{\sqrt{\kappa\gamma_\parallel}} B(T) e^{i[(1+\omega_c)t + kx]} \begin{pmatrix} 1 \\ -\dfrac{2\Delta\kappa}{(\kappa+\gamma_\perp)} + i2\kappa \\ 0 \end{pmatrix}$$
$$+ o(\epsilon^3). \tag{5}$$

The quadratic amplitude equations take the form

$$\partial_t A = \mu A + e^{i\alpha}(N_0 A + \overline{N}_2 B),$$
$$\partial_t B = \mu B + e^{i\alpha}(N_0 B + N_2 A),$$
$$\partial_t N_2 = -N_2 - \overline{A} B, \tag{6}$$
$$\partial_t N_0 = -N_0 - \{\ |A|^2 + |B|^2\},$$

where $\mu = \tilde{\mu}/\gamma_\parallel$.

These amplitude equations possess solutions which are easily identified as follows: (i) Traveling waves (TW) which describe the propagation of a pure left- or right-going wave; (ii) mixed waves (MW), which are the superposition of right- and left-traveling waves with different amplitudes; (iii) standing waves (SW), which correspond to the superposition of right- and left-traveling waves with equal amplitudes; (iv) periodic alternating waves (PAW), which represent a time-dependent periodic oscillation of the amplitudes of the right- and left-going wave amplitudes; (v) chaotic alternating waves (CAW), which represent a time-dependent chaotic oscillation of the amplitudes of the right- and left-going wave amplitudes. TW, MW, and SW solutions have simple analytical expression, while PAW can be only obtained approximately, close to the parameter value where they bifurcate from SW. CAW are computed numerically. Their existence can be deduced from general results of the dynamical systems theory.

Right-going TW solutions are given by

$$A = R\exp[-i(\mu\tan\alpha)t], \quad B=0, \quad N_0=0, \quad N_2=-R^2, \tag{7}$$

where $R=\mu/\cos(\alpha)$ and a similar expression where A and B are exchanged for the left-going traveling waves. TW solutions are stable for small μ, since N_0 and N_1 can be adiabatically eliminated in this parameter range. The adiabatic elimination fails close to $\alpha=\pi/2$ because the real part of the reduced equation vanishes. TW lose their stability on a line noted I_{TW} ($\mu=\cot^2\alpha$) in Fig. 1. This bifurcation leads to the appearance of MW solutions.

The study of the other solutions simplifies if one uses the following change of variables which reduces the dimension of the dynamical system from seven to five: $A \equiv R\cos(\phi/2)e^{i\theta}$, $B\equiv R\sin(\phi/2)e^{i\varphi}$, $N_2\equiv Se^{i\chi}$, $N_0=N$, and $\zeta\equiv\varphi-\theta-\chi$. The reduced amplitude equations then read

$$\partial_t R = [\mu + N\cos(\alpha)]R + SR\sin(\phi)\cos(\alpha)\cos(\zeta),$$
$$\partial_t \phi = 2S\sin(\alpha)\sin(\zeta) + 2S\cos(\phi)\cos(\alpha)\cos(\zeta),$$
$$\partial_t S = -S - \frac{R^2}{2}\sin(\phi)\cos(\zeta), \tag{8}$$

$$\partial_t N = -N - R^2,$$
$$\partial_t \zeta = S \cot\left(\frac{\phi}{2}\right)\sin(\alpha-\zeta) - S \tan\left(\frac{\phi}{2}\right)\sin(\alpha+\zeta) + \frac{R^2}{2S}\sin(\phi)\sin(\zeta).$$

MW solutions are explicitly given by

$$A \equiv R\cos\left(\frac{\phi}{2}\right)e^{i\theta}, \quad B \equiv R\sin\left(\frac{\phi}{2}\right)e^{i\varphi},$$
$$N_0 \equiv S e^{i\chi}, \quad N_2 = -R^2,$$

where

$$R^2 = \frac{\mu}{\left(1+\frac{\sin(\phi)^2\cos(\zeta)^2}{2}\right)\cos(\alpha)},$$
$$S = -\frac{R^2}{2}\sin(\phi)\cos(\zeta),$$
$$\cos^2(\phi) = \frac{\sin(\alpha)^2[2\mu - 3\cos(\alpha)^2]}{\cos(\alpha)^2[3\cos(\alpha)^2-1]}, \tag{9}$$
$$\tan^2(\zeta) = \frac{2\mu-3\cos(\alpha)^2}{[3\cos(\alpha)^2-1]},$$

and $\zeta \equiv \varphi - \theta - \chi$. MW bifurcate from TW on the curve $\mu = \cot^2\alpha$ and from SW on the curve I_{SW} $(\mu = \frac{3}{2}\cos^2\alpha)$. The bifurcation from SW is a pitchfork bifurcation corresponding to the breaking of the parity symmetry $(x \to -x)$. The bifurcation changes from supercritical to subcritical at the tricritical point noted by $\alpha = \arccos(1/\sqrt{3})$ and $\mu = \frac{1}{2}$.

SW solutions are given by

$$A \equiv R\frac{\sqrt{2}}{2}e^{i\theta}, \quad B \equiv R\frac{\sqrt{2}}{2}e^{i\varphi}, \quad N_0 \equiv S e^{i\chi}, \quad N_2 = -R^2,$$

where

$$R^2 = \frac{2\mu}{3\cos(\alpha)}, \quad S = -\frac{R^2}{2}$$
$$\phi = \pm\frac{\pi}{2}, \quad \varphi - \theta - \chi = 2n\pi. \tag{10}$$

SW lose their stability in two different ways, as follows.

(i) On the line I_{SW} $(\mu = \frac{3}{2}\cos^2\alpha)$, their instability leads to the appearance of MW through a pitchfork bifurcation. The symmetry-breaking amplitude x is defined by

$$\begin{pmatrix}\phi\\ \zeta\end{pmatrix} = x\begin{pmatrix}\sin\alpha\\ \cos\alpha\end{pmatrix} + \left\{\frac{2}{3}\eta\frac{\tan\alpha}{\cos\alpha}x + \frac{x^3}{6}\sin\alpha\cos\alpha \times(2\cos^4\alpha - 5\cos^2\alpha+1)\right\}\begin{pmatrix}\cos\alpha\\ \sin\alpha\end{pmatrix} + (\text{higher-order terms}) \tag{11}$$

and

$$R^2(\phi,\zeta) = -N(\phi,\zeta) = \frac{2\mu}{\cos\alpha(2+\cos^2\phi\cos^2\zeta)},$$
$$S(\phi,\zeta) = -\frac{\mu\cos\phi\cos\zeta}{\cos\alpha(2+\cos^2\phi\cos^2\zeta)}. \tag{12}$$

It satisfies the amplitude equation

$$\dot{x} = \frac{1}{\cos^2\alpha - \sin^2\alpha}\left\{\frac{2}{3}\eta x - \cos^2\alpha(3\cos^2\alpha - 1)\frac{x^3}{3}\right\}, \tag{13}$$

with $\eta = \mu - \frac{3}{2}\cos^2\alpha$.

(ii) On the line I_{PAW} $(\mu = \frac{3}{4},\ \alpha \geqslant \pi/4)$, the instability of SW leads to a stable limit cycle through a supercritical Andronov-Hopf bifurcation. The amplitude of the PAW is defined as

$$\begin{pmatrix}\phi\\ \zeta\end{pmatrix} = \left\{A + \left(-\frac{\eta}{3} + i\frac{\eta}{12\Omega^2\sin^2\alpha}\right)\overline{A} + \frac{(1-\cos^4\alpha)+2i\Omega(\cos^2\alpha - \cos^4\alpha)}{48\Omega^2\sin^2\alpha\cos^2\alpha}A^3 - \frac{(7+37\cos^4\alpha - 28\cos^2\alpha)+i\Omega(22\cos^4\alpha - 6\cos^2\alpha)}{48\Omega^2\sin^2\alpha\cos^2\alpha} \times |A|^2\overline{A} + \frac{(5\cos^2\alpha+1)+4i\Omega(\cos^4\alpha-\cos^2\alpha)}{96\Omega^2\sin^2\alpha\cos^2\alpha} \times\overline{A^3}\right\}\begin{pmatrix}1\\ \cot\alpha(1-i2\Omega)\end{pmatrix} + \text{c.c.} + (\text{higher-order terms}) \tag{14}$$

and

$$R^2(\phi,\zeta) = -N(\phi,\zeta) = \frac{2\mu}{\cos\alpha(2+\cos^2\phi\cos^2\zeta)},$$
$$S(\phi,\zeta) = -\frac{\mu\cos\phi\cos\zeta}{\cos\alpha(2+\cos^2\phi\cos^2\zeta)}. \tag{15}$$

It obeys the amplitude equation

$$\partial_t A = \left(\frac{\eta}{6\Omega\sin^2\alpha} - i\frac{2\Omega\eta}{3}\right)A - i\frac{(7+23\cos^4 a - 30\cos^2\alpha)}{24\Omega\cos^2\alpha\sin^2\alpha}|A|^2 A - \frac{8\Omega(\cos^2\alpha - \cos^4\alpha)}{24\Omega\cos^2\alpha\sin^2\alpha}|A|^2 A, \tag{16}$$

where $\Omega = \sqrt{\tan^2\alpha - 1}/2$ and $\eta = \mu - \frac{3}{4}$.

The two bifurcations interact at the point $\mu = \frac{3}{4}$, $\alpha = \pi/4$, where the two bifurcation lines intersect. This point corresponds to a codimension-2 Bogdanov-Takens bifurca-

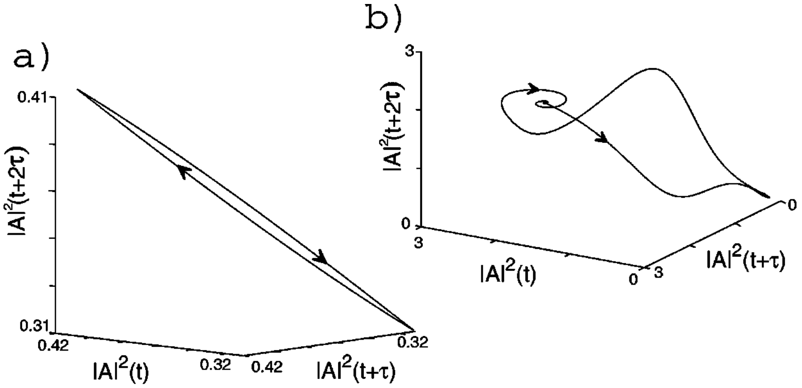

FIG. 2. Reconstructed phase portrait using the amplitude of the right-going wave ($\tau=5$). (a) Parameters close to the Bogdanov Takens codimension-2 bifurcation. (b) Parameters close to the instability line of traveling wave $I_{\rm TW}$.

tion. Close to $\mu=\frac{3}{4}$, $\alpha=\pi/4$, the five-dimensional amplitude equations reduces to a second-order differential equation,

$$\ddot{x}=\frac{4}{3}(\varepsilon-2x^2)\dot{x}-\left(\eta+\frac{2}{3}\varepsilon\right)x+\frac{x^3}{6}, \tag{17}$$

where $\epsilon=\mu-\frac{3}{4}$, $\eta=\alpha-(\pi/4)$, and

$$\begin{aligned}\begin{pmatrix}\phi\\ \zeta\end{pmatrix}&=\left[x+\left(\frac{4\epsilon}{3}+2\eta\right)x\right]\begin{pmatrix}1\\1\end{pmatrix}+\left(-\frac{x^3}{9}+\frac{x^2\dot{x}}{6}+\frac{2}{3}x\dot{x}^2\right)\begin{pmatrix}1\\1\end{pmatrix}\\&\quad+\left[\dot{x}-\left(\frac{4\epsilon}{3}+2\eta\right)x\right]\begin{pmatrix}2\\0\end{pmatrix}+\left(\frac{7}{3}x^3-\frac{5}{3}x^2\dot{x}-x\dot{x}^2\right)\begin{pmatrix}2\\0\end{pmatrix}\\&\quad+\text{higer-order terms}\end{aligned} \tag{18}$$

and

$$\begin{aligned}R^2(\phi,\zeta)&=-N(\phi,\zeta)=\frac{2\mu}{\cos\alpha(2+\cos^2\phi\cos^2\zeta)},\\ S(\phi,\zeta)&=-\frac{\mu\cos\phi\cos\zeta}{\cos\alpha(2+\cos^2\phi\cos^2\zeta)}.\end{aligned} \tag{19}$$

The unfolding of this codimension-2 bifurcation contains SW and MW solutions and the PAW solution and their bifurcations. A particularly interesting bifurcation, which further organizes the parameters space occurs when the limit cycle (PAW) becomes a heteroclinic loop [13] which connects the MW solutions. Close to the bifurcation, the alternation period diverges logarithmically. The line $\mu=-4\alpha$, where the Andronov heteroclinic bifurcation occurs, can be continued numerically as it is shown in Fig. 1. For large values of μ this line coincides asymptotically with the TW-MW transition line. The Jacobian operator evaluated at the MW solution, for parameters values corresponding to the Andronov bifurcation, possesses three real eigenvalues λ_+, λ_1, and λ_2 and a complex one λ_c. These eigenvalues control the topology of the limit cycle and its stability in the neighborhood of the Andronov bifurcation. In the vicinity of the codimension-2 bifurcation, $\lambda_+>0>\lambda_1>\mathrm{Re}(\lambda_c)>\lambda_2$ and $|\lambda_+|<|\lambda_1|$; the PAW solution is stable and connects MW solutions in a monotonous way [see Fig. 2(a)]. Above the point noted $S(\mu=0.856,\ \alpha=0.7553)$ in Fig. 1 one has $\lambda_+>0>\mathrm{Re}(\lambda_c)>\lambda_1>\lambda_2$ and $|\lambda_+|<|\mathrm{Re}(\lambda_c)|$. In this range of parameters, the limit cycle is stable, but it connects the MW solutions with damped oscillations [see Fig. 2(b)]. Thus the heteroclinic bifurcation appears to be of Shilnikov type in this case. Since the limit cycle is stable, chaotic behaviors are ruled out in the vicinity of the heteroclinic bifurcation [14] as Fig. 3 shows. Nevertheless, chaotic behavior characterized by the formation of multiple horseshoes can be expected at a finite distance from the heteroclinic bifurcation. These chaotic behaviors are indeed observed numerically [cf. Fig. 3(b)]. Experimentally, under certain conditions periodic doubling route chaos was observed [5]. By increasing the detuning, while fixing the pump parameter, one observes the following scenario: in a very limited range of variation of the detuning one observes stable traveling waves which become unstable and give rise to PAW. If one continues to increase the detuning, one then observes the transition towards CAW. Finally, a too large detuning extinguishes the laser after a regime in which stable standing waves should be observed.

The difficulties in analyzing the Maxwell-Bloch equations using amplitude equations come from the quasireversible nature of the problem [15]. The degeneracy of reversible systems is generally removed when the damping and forcing are taken into account. Here we have privileged a simple asymptotic limit which contains many of the phenomena observed in real experiments. Some important aspects are missing, nevertheless, as, for example, the damped oscillations generally observed near the laser threshold [5,9]. A simple way to recover these important aspects consists in considering a more general asymptotic limit in which all damping coefficients are of the same order of the distance from threshold. Within this new asymptotic, the amplitude equations read

$$\begin{aligned}\partial_{tt}A&=\mu A-(\kappa+i\Delta)\partial_tA+e^{i\alpha}(N_0A+\overline{N}_2B),\\ \partial_{tt}B&=\mu B-(\kappa+i\Delta)\partial_tB+e^{i\alpha}(N_0B+N_2A),\\ \partial_tN_2&=-N_2-\overline{A}B,\\ \partial_tN_0&=-N_0-\{|A|^2+|B|^2\}.\end{aligned} \tag{20}$$

Obviously these equations contain richer dynamical behaviors since they reduce to the amplitude equations discussed in this paper in the limit $\gamma_\parallel+\kappa\gg\gamma_\perp$.

III. CONCLUSION

We have reduced asymptotically the Maxwell-Bloch equation to a simple set of quadratic amplitude equations characterized by two parameters. This model allows us to

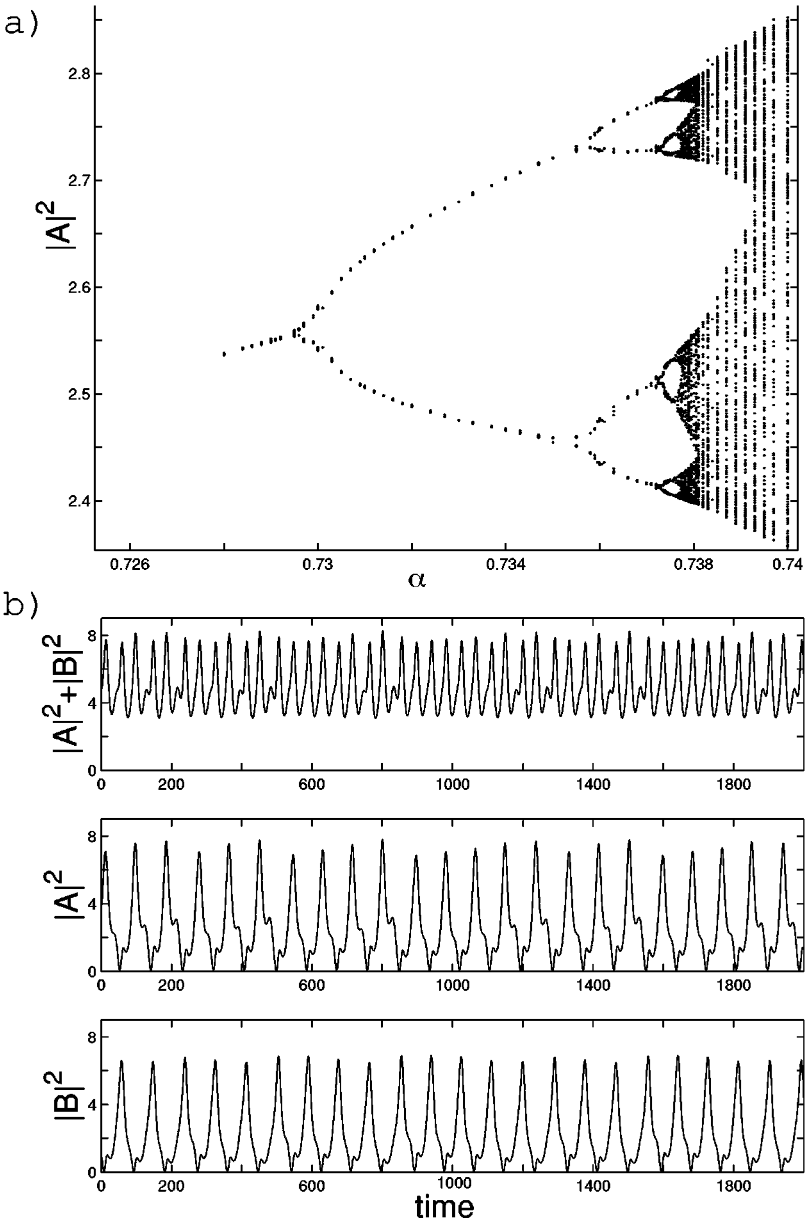

FIG. 3. (a) Projection of the Poincaré map defined by a constant amplitude of the left-going wave ($B=1$) for $\mu=4$. (b) Temporal signal of the intensity of $|A|^2+|B|^2$, $|A|^2$, and $|B|^2$ in the chaotic regime ($\alpha=0.74$, $\mu=1$).

study in detail the mechanism of the transition from traveling waves to alternating waves and the nature of the chaotic behaviors. The validity of the set of quadratic amplitude equations includes the class *C* laser, where we also have a qualitative agreement with the experiments [5].

ACKNOWLEDGMENTS

The authors acknowledge Cátedra Presidencial and the EU through a TMR grant FMRX-CT96-0010. One of us (P.C) acknowledges the support of the ''Institut Universitaire de France.''

[1] A. Newell and J. Moloney, *Nonlinear Optics* (Addison-Wesley, Redwood, CA, 1992).
[2] F. Aronowitz, in *Laser Applications*, edited by M. Ross (Academic, New York, 1971), Vol. 1, p. 133.
[3] P. Khandokhin and Ya. Khanin, J. Opt. Soc. Am. B **2**, 226 (1985).
[4] J. White, Phys. Rev. **137**, A1651 (1965).
[5] D. Y. Tang, R. Dykstra, and N. R. Heckenberg, Opt. Commun. **126**, 318 (1996).
[6] D. Y. Tang, M. Li, J. Malos, N. R. Heckenberg, and C. Weiss, Phys. Rev. A **52**, 717 (1995).
[7] D. Y. Tang, J. Pujol, and C. Weiss, Phys. Rev. A **44**, 717 (1991).
[8] G. Lippi, J. Tredicce, N. Abraham, F. Arecchi, Opt. Commun. **53**, 129 (1985).
[9] N. V. Kravtsov and E. G. Lariontsev, Quantum Electron. **24**, 841 (1994).
[10] H. Zeghlache, P. Mandel, N. B. Abraham, L. M. Hoffer, G.L. Lippi, and T. Mello, Phys. Rev. A **37**, 470 (1988).
[11] L. M. Hoffer and N. B. Abraham, Opt. Commun. **74**, 261 (1986).
[12] A. E. Seigman, *Laser* (University Science Books, Mill Valley,

1986).

[13] J. Guckenheimer and P. Holmes, *Nonlinear Oscillations, Dynamical System and Bifurcations of Vector Fields* (Springer-Verlarg, New York, 1983).

[14] A. Arneodo, P. H. Coullet, E. A. Spiegel, and C. Tresser, Physica D **14**, 327 (1985); L. P. Shil'nikov, Math. U.S.S.R. Sbornik **6**, 427 (1968).

[15] M. Clerc, P. Coulet, and E. Tirapegui, Phys. Rev. Lett. (to be published).